

Quasi-exotic open-flavor mesons^a

T. Hilger^{b,1}, A. Krassnigg^{c,1}

¹Institute of Physics, University of Graz, NAWI Graz, A-8010 Graz, Austria

Received: June 14, 2021/ Accepted: date

Abstract Meson states with exotic quantum numbers arise naturally in a covariant bound-state framework in QCD. We investigate the consequences of shifting quark masses such that the states are no longer restricted to certain \mathcal{C} -parities, but only by $J^{\mathcal{P}}$. Then, *a priori*, one can no longer distinguish exotic or conventional states. In order to identify signatures of the different states to look for experimentally, we provide the behavior of masses, leptonic decay constants, and orbital-angular-momentum decomposition of such mesons, as well as the constellations in which they could be found. Most prominently, we consider the case of charged quasi-exotic excitations of the pion.

Keywords Meson spectroscopy · Bethe-Salpeter equation · Dyson-Schwinger equations · exotic states · orbital angular momentum

PACS 14.40.-n · 12.38.Lg · 11.10.St

1 Introduction

The appeal of discovering the patterns of mesons with exotic quantum numbers [1] comes from the same source as the term *exotic* itself, namely the quark-model picture [2–4]. Mesons are classified via their total angular momentum J , parity \mathcal{P} , and, if the state can be seen as its own antiparticle, by charge-conjugation parity \mathcal{C} . In the quark-model setup, one combines one quark and one antiquark with total spin s and orbital angular momentum l to get a meson with $J^{\mathcal{P}\mathcal{C}}$, where $\mathcal{P} = (-1)^{l+1}$, $\mathcal{C} = (-1)^{l+s}$, and $|l-s| \leq J \leq |l+s|$. Any combination of $J^{\mathcal{P}\mathcal{C}}$ that violates these constraints is termed *exotic*.

^aThis work was supported by the Austrian Science Fund (FWF) under project no. P25121-N27.

^be-mail: thomas.hilger@uni-graz.at

^ce-mail: andreas.krassnigg@uni-graz.at

Indeed, the patterns of meson states predicted by the quark model matched those found in experiment. Exotic states do not seem to appear in the experimental meson spectrum with the exception of the isovector 1^{-+} case [5–14, 14, 15, 15–18]. Since even those states are under debate, both systematic experimental evidence for states with exotic quantum numbers as well as a sound theoretical concept and understanding of their peculiarities are among the top priorities of modern hadron physics [19].

Still, it is puzzling that there should be such a profound conceptual difference between exotic and conventional mesons from the point of view of a covariant bound-state amplitude, since there the above restrictions do not apply. In particular, a Poincaré covariant formulation of the two-body bound-state problem additionally has a relative time freedom of the constituents and thus lifts the nonrelativistic $J^{\mathcal{P}\mathcal{C}}$ limitations [20]. For a quark bilinear Bethe-Salpeter amplitude (BSA), one has three four-vectors and their scalar products as building blocks: the total momentum P , the $\bar{q}q$ relative momentum k , and the four vector of Dirac matrices γ as a representation of the direct spinor product [21–23].

For example, a scalar BSA has four possible independent covariants:

$$\mathfrak{t}_j \in \{\mathbf{1}, \gamma \cdot P, \gamma \cdot k, -\frac{1}{2} [\gamma \cdot k, \gamma \cdot P]\}_{j=1,2,3,4}, \quad (1)$$

where $\mathbf{1}$ is the unit matrix in Dirac space. The BSA for $J^{\mathcal{P}} = 0^+$ is obtained as

$$\Gamma(k; P; \gamma) := \sum_{i=1}^4 \mathfrak{t}_i(k; P; \gamma) F_i(k^2, k \cdot P, P^2), \quad (2)$$

the generalization to other $J^{\mathcal{P}}$ is straightforward [24]. The invariant amplitudes F_i are parameterized in terms of the Lorentz-invariants P^2 , k^2 , and $k \cdot P$. There is no *a priori* restriction of \mathcal{C} at this point. While each covariant \mathfrak{t}_i has a definite \mathcal{C} -parity, the dependence of the F_i on $k \cdot P$, which has

$\mathcal{C} = -1$ in contrast to P^2 and k^2 , allows for both $\mathcal{C} = \pm 1$ of the BSA. The construction of Eq. (2) is also valid for the case of an open-flavor meson [25–31], where the F_i do not possess a definite symmetry regarding $k \cdot P$. A covariant approach thus allows for any set of $J^{\mathcal{P}\mathcal{C}}$ without the explicit appearance of gluonic or other degrees of freedom additional to quark bilinears [32–36].

The most common starting point to address an exotic state is the notion of *hybrid* mesons, which *explicitly* contain some gluonic excitation. Hybrid-meson supermultiplets contain states with both exotic and conventional quantum numbers and have different content and properties, depending on the method of investigation. In a recent article [37], lattice results [38, 39] were partly contrasted to various different model setups [40–46]. The results for mass ranges of the hybrid supermultiplets described there vary as does the candidate for the lightest meson with exotic quantum numbers. The majority of investigations finds them close to or above 2 GeV, and the lightest is, e. g., the $J^{\mathcal{P}\mathcal{C}} = 1^{-+}$ [47], or the 0^{-+} [48].

In the Dyson-Schwinger-Bethe-Salpeter-equation (DS-BSE) approach, exotic mesons have been studied in detail some time ago in the context of the 1^{-+} channel [20], which was also part of our recent line of investigations [49–52], and for $J = 0, 1$ in [53]. Still, herein we present the first systematic set of predictions and conclusions for such states in our approach, which are anchored to some of QCD’s model-independent properties, in particular the behavior of the isovector pseudoscalar meson ground-state mass and leptonic decay constant as well as the leptonic decay constants of all its excitations in the chiral limit. The corresponding excited-state masses, on the other hand, are not anchored to QCD properties, since they are not constrained by the axial-vector Ward-Takahashi identity. This provides freedom and predictive power for the model calculation in the sense that these masses vary strongly with changes in some model parameters and can be used to test and falsify our results.

Irrespective of the approach and the construction with respect to gluonic degrees of freedom used to describe mesons, one faces a very interesting situation in the open-flavor case. Since such states are not restricted by \mathcal{C} , one needs criteria, signals, or simply hints as to whether some of these states have exotic characteristics, i. e., do not exist in the quark model, and which ones. Clearly, one can expect some kind of similarity or correspondence of open-flavor states and certain quarkonia.

Concretely, as illustrated in Fig. 1, one can approach the case of a \mathcal{C} -eigenstate from the perspective of a meson with strangeness $\bar{n}s$, both towards the $\bar{n}n$ and $\bar{s}s$ limits. This is based on the reasonable notion that, when varying quark masses, mass trajectories of corresponding meson bound states should be continuous and no states should disappear or appear. We use the term *quasi-exotic* for flavored

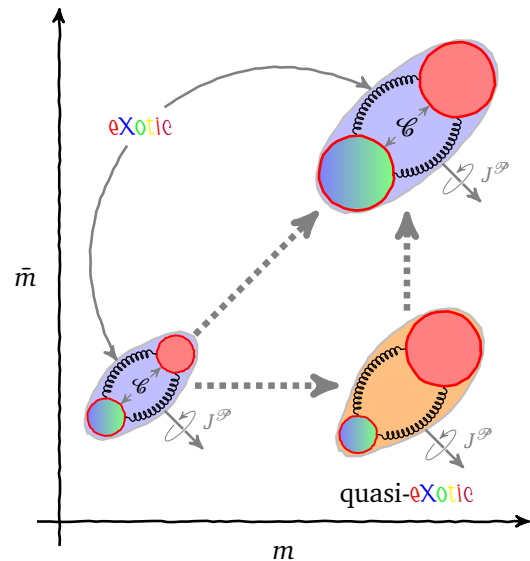


Fig. 1 Schematics of the connection of exotic and quasi-exotic mesons.

mesons that can be connected to exotic \mathcal{C} -eigenstates. We argue that such states do not exist in the quark model, similar to exotic states. As it turns out, the most prominent and probably most characteristic instance of a quasi-exotic meson could be an excited charged pion.

Note that mesons in QCD are strong resonances above the respective decay thresholds. While this is a qualitative difference to the bound-state picture used herein as a result of the fact that there are no strong decay mechanisms in the truncated used as described below, we do not expect a model calculation to be inexplicably discontinuous as a function of the current-quark mass, even if it does include hadronic decay channels. Thus, our qualitative argument does not suffer from this omission. Nevertheless, a treatment of meson states as resonances, where applicable, is a necessary next step in model calculations such as ours.

2 Properties of mesons in QCD

The Dyson-Schwinger equations (DSEs) of QCD are the equations of motion in this quantum field theory [54], a general concept easily extendable, e. g., to finite temperature and density [55–61]. Their complete solution amounts to a solution of QCD in terms of the dynamics of quarks and gluons; however, this task is highly nontrivial [62–69]. While numerical studies such as ours require a truncation of this infinite tower of coupled nonlinear integral equations, some results can be obtained in a truncation-independent manner, since they are connected to (broken) symmetries of QCD and are realized through Ward-Takahashi identities (WTIs) or Slavnov-Taylor identities [70].

Such a truncation-independence of meson properties is basically qualitative of nature, but also quantitative in the sense that a value of zero is precisely reproduced and values close to a corresponding point or limit are also quantitatively reliable, if properly anchored via appropriate choices for the model parameters. In our case, we concretely have the exact behavior in the chiral limit of meson properties as described above. Thus, for small quark masses, our calculated values for the corresponding anchored mass or leptonic decay constant should also be reliable. The properties and relations considered regarding this feature are described in the following. Our results are presented with a clear qualitative focus and a quantitative note, where we mention experimental values.

A prime example is the axial-vector WTI which is connected to QCD's chiral symmetry and the both dynamical and explicit breaking thereof [71–76]. If a truncation, such as the RL truncation used here, satisfies this WTI, all aspects of chiral symmetry and its dynamical breaking are realized in the model by construction. In particular, the pion ground state becomes massless in the chiral limit, where it is identified as the Goldstone boson connected to dynamical chiral symmetry breaking (DCSB). Further well-known relations appear as consequences of WTIs, such as the Gell-Mann-Oakes-Renner relation. A generalized form of the latter [77] can be written together with a similar relation for scalar mesons [53] as

$$f_{0\mathcal{P}} M_{0\mathcal{P}}^2 = (m_q - \mathcal{P} m_{\bar{q}}) r_{0\mathcal{P}}, \quad (3)$$

which provides both model independent insight as well as a means to check numerical studies. $f_{0\mathcal{P}}$ and $M_{0\mathcal{P}}$ are the meson's leptonic decay constant and mass, respectively, $m_{(\bar{q})q}$ are the current-(anti)quark masses, and $r_{0\mathcal{P}}$ is a projection of, e. g., the pseudoscalar BSA on a pseudoscalar current instead of the axialvector that defines f_{0-} [25].

For pseudoscalar mesons it is known [78–80] and established also in the DSBSE approach [81] via Eq. (3) that leptonic decay constants of all radially excited pseudoscalar mesons are zero in the chiral limit, if one has DCSB. For realistic light-quark masses one arrives at values of the order of $f_\pi \approx 1 - 10$ MeV for the first radial excitation of the pion both in the DSBSE and other approaches [81–86]. While all radially excited pseudoscalar mesons have a small leptonic decay constant compared to the pion ground state's, exotic 0^{--} excitations have a vanishing decay constant as a direct result of the projection onto the axialvector current.

For scalar mesons, it is evident from Eq. (3) that the projection f_{0+} of a scalar BSA on a vector current vanishes for all states with $m_q = m_{\bar{q}}$ irrespective of their level of excitation, including exotic 0^{+-} quantum numbers [53, 87]. For vector mesons their leptonic decay constant f_{1-} [88] is generally nonzero for conventional and zero for exotic states.

Our numerical investigation is based on these boundary conditions, which are satisfied to high accuracy.

3 Essentials of model setup

RL truncation combines the rainbow truncation of the quark DSE with the ladder truncation of the $\bar{q}q$ BSE via an effective model quark-gluon interaction [25, 88]. First, the quark DSE is solved numerically and prepared as an input to the meson BSE [24, 26, 89–91], which is then solved numerically as well via well-established techniques [92–94]. The quark dressing functions follow typical patterns of DCSB in QCD [95, 96].

Instead of using a Chebyshev expansion for the F_i (for an illustration see [53, 94, 97]) and having to keep many Chebyshev moments, we retain the full angular dependence in our calculation as it was pioneered and detailed in [25, 88] together with the usual convergence checks for numerically discretized integration in order to preserve independence from the $\bar{q}q$ momentum partitioning [98] demanded by Poincaré covariance. Varying the partitioning in open-flavor DSBSE calculations [26] allows us to sample quark propagators only on their analytic domain [99] and to directly solve the homogeneous BSE, obtaining the masses and leptonic decay constants shown in Fig. 2. Note that exotic meson masses are underestimated in RL truncation if compared to other approaches, but are shifted up by corrections beyond RL, as one must expect, see [100] and references therein.

Unless noted otherwise, we use the model of Ref. [88], which has the correct UV limit of perturbative QCD and an intermediate-momentum enhancement producing DCSB parameterized by an inverse effective range ω and an overall strength D . Our values $\omega = 0.3$ GeV, $D = 1.3$ GeV² are chosen close to one of the original sets [88] aimed at our particular purposes of this study: a rich data set and the exact boundary conditions described above.

To ensure high-quality numerical results and reduce the chance of error as much as possible, we leave very little room for manual errors by high automatization of the calculational setup. In particular, we employ configuration-consistency checks, various plausibility and consistency checks at the level of the results, qualitative and quantitative data checks, and use automatic data visualization for a manual data check, when necessary.

4 Results and discussion

We investigate the m_q and subsequent $m_{\bar{q}}$ evolution of the meson masses and leptonic decay constants of the ground state as well as two excited states for $J^{\mathcal{P}} = 0^-, 0^+, 1^-$,

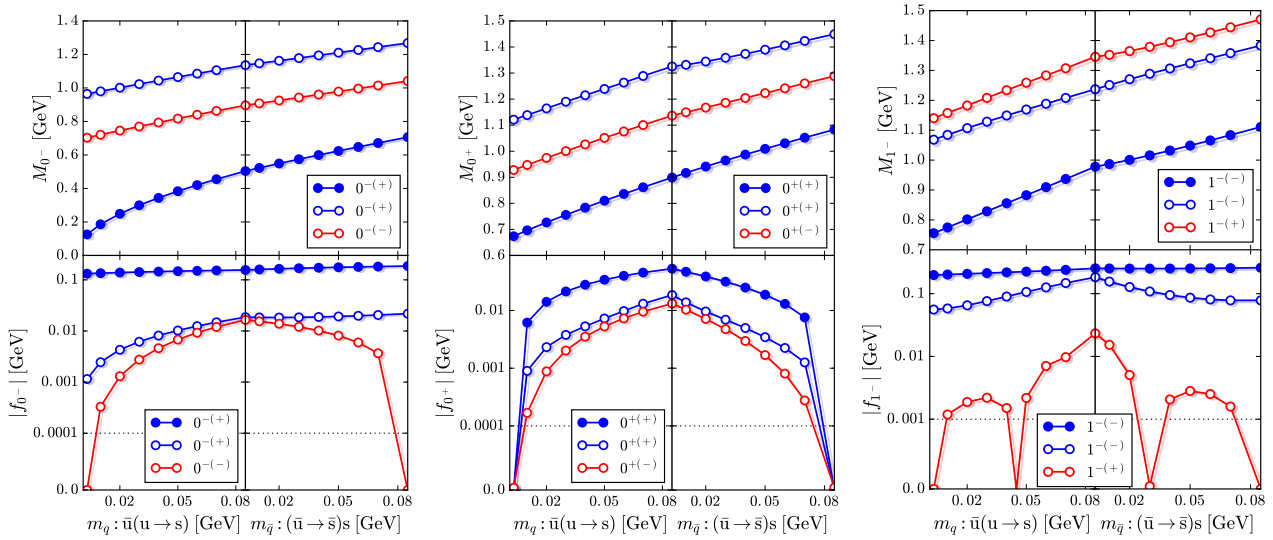


Fig. 2 Masses (*top*) and decay constants (*bottom*) as functions of quark masses; left half of each figure: quark mass increases from light to strange; right half of each figure: antiquark mass increases from light to strange. *From left to right*: pseudoscalar, scalar, and vector. Below the dotted line, the vertical axis is linear instead of logarithmic.

where one excitation is connected to exotic and one to conventional \mathcal{C} -eigenstates. The quantum numbers $J^{\mathcal{P}(\mathcal{C})}$ of each state together with a continuity requirement for the meson masses, decay constants, orbital angular momentum properties, and relation (3) are utilized to uniquely identify and assign conventional and quasi-exotic open-flavor states to their conventional and exotic \mathcal{C} -eigenstate counterparts.

The light and strange quark masses are fitted to the experimental values of the π and K mesons' leptonic decay constants, $f_{\pi^-} = 0.13041(20)$ and $f_{K^-} = 0.1562(7)$ GeV [101]. At our renormalization point of $\mu = 19$ GeV [25], $m_n(\mu) = 0.003$ and $m_s(\mu) = 0.085$ GeV, which yield the calculated $f_{\pi^-} = 0.132$ and $f_{K^-} = 0.156$ GeV, respectively.

We present our results in Fig. 2. The first excitation in our model setup is exotic (red) and the second conventional (blue). For the 1^- case, we show higher excitations (whose order is reversed), since for the first two continuous mass curves cannot be produced because between the $\bar{n}n$ and $\bar{s}s$ cases the homogeneous BSE does not produce real eigenvalues for these states at some point. This is a non-numerical problem encountered typically in open-flavor DSBSE model calculations [28] and is under current investigation also for states representing baryons [102] or with equal-mass constituents [103]. However, this behavior does not pertain to our argument, since our focus is the association of exotic and quasi-exotic states.

The leptonic decay constants are presented in the lower row of Fig. 2, where we plot $|f|$ in each case, since f has alternating positive and negative signs for a tower of radial excitations [81, 104, 105]. The accurate realization of the exact boundary conditions given above is perfectly visible

for the scalar case (middle), where all values for f drop to zero in both $\bar{q}q$ limits.

For the pseudoscalars, the situation is a bit more subtle: In the presence of DCSB, the ground-state pion's decay constant is sizeable and, when increasing one quark mass to the strange quark's value, rises slowly to the corresponding value for the K . The first conventional excitation has $f \approx 1$ MeV, which is two orders of magnitude smaller than for the ground state and only nonzero as a result of explicit chiral symmetry breaking by the current light-quark mass.

The first $\bar{n}n$ exotic pseudoscalar has an f of exactly zero. Interestingly, if other studies of hybrids with exotic quantum numbers find a small but finite value for f , this provides an excellent way to test such hypotheses against ours.

With one quark mass increasing to m_s , both excitations' values for f increase to a number of just under 20 MeV, which means that in the strange sector, according to our picture, a kaon excitation expected from the quark model would be indistinguishable from the quasi-exotic state we show here on the basis of their leptonic decay constants.

However, there is a prominent case where f provides a clear signal to distinguish conventional and quasi-exotic states: excited charged pions. While herein we compute the pion's properties on the basis of equal u and d quark masses as well as isospin symmetry, and also neglect electromagnetic effects on the different charge states, we can still conclude that a charged excited pion connected to a conventional state should have $f \approx 1$ MeV as well, while quasi-exotic charged pions have $f \approx 0.1$ MeV, i. e., one order of magnitude smaller. This can be seen from the first data point from the left in the lower left subfigure of Fig. 2, which corresponds to a possible current-quark mass combination for

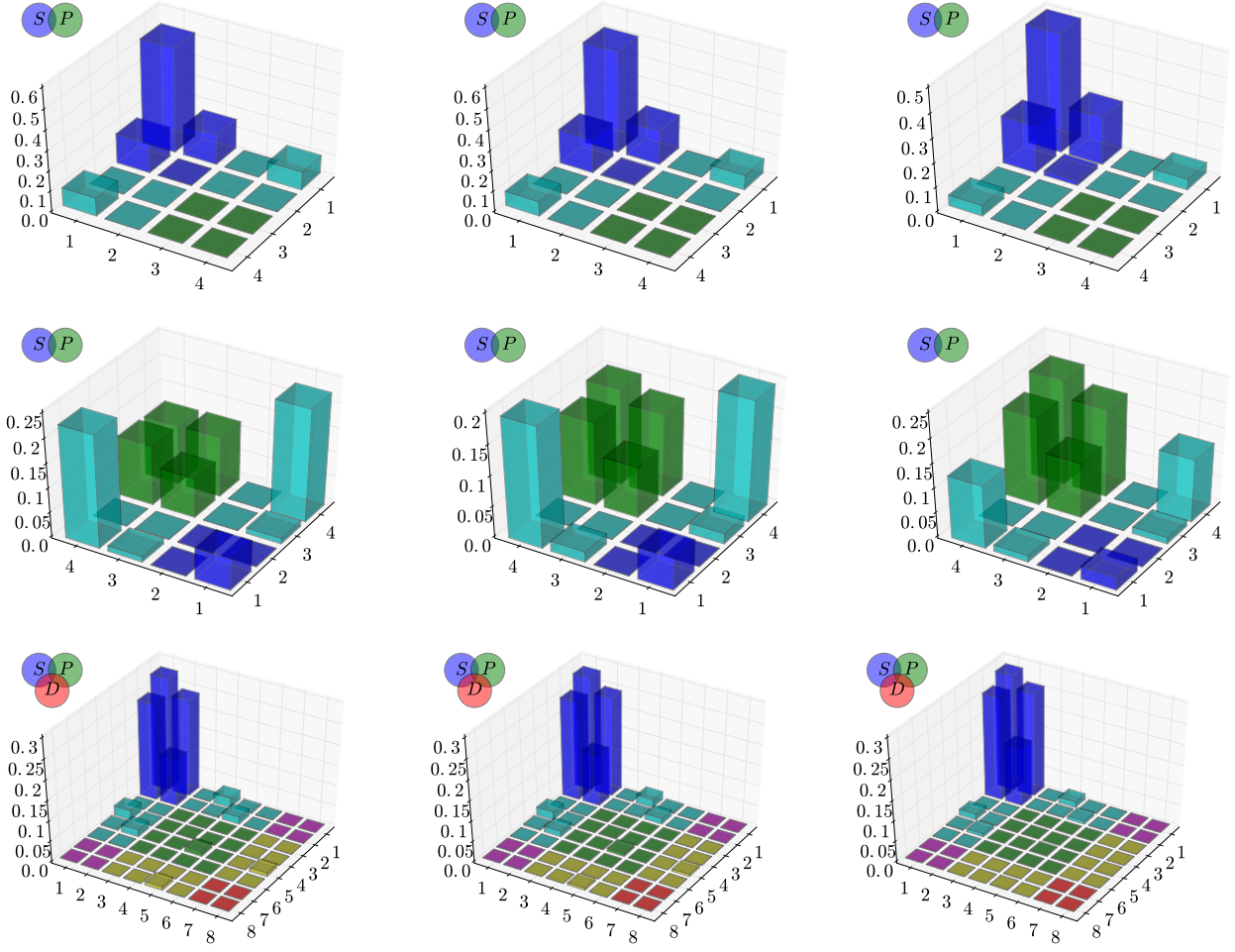


Fig. 3 Orbital angular momentum contributions to the BSA's canonical norm for ground states. The rows in the figure correspond to key points on the graphs in Fig. 2 as follows (states in notation flavor- $n(J^{\mathcal{P}(\ell)})$): *Upper row*: $\bar{u}u$ - $0(0^+)$, $\bar{u}s$ - $0(0^-)$, $\bar{s}s$ - $0(0^+)$; *Center row*: $\bar{u}u$ - $0(0^{++})$, $\bar{u}s$ - $0(0^+)$, $\bar{s}s$ - $0(0^{++})$; *Lower row*: $\bar{u}u$ - $0(1^{--})$, $\bar{u}s$ - $0(1^-)$, $\bar{s}s$ - $0(1^{--})$.

a realistic charged pion. Finding a state with such a quasi-exotic signature would thus immediately signal the existence of exotic 0^{--} pseudoscalars of about the same mass. More precisely, the existence of a quasi-exotic state implies the existence of two more associated exotic states.

The argument obviously works both ways, and so the existence of quasi-exotic states can also be inferred from the exotic case. This is an interesting statement for the case of the 1^{--} as shown in Fig. 2. The ground-state values of f_ρ and f_ϕ are connected by a slow and steady increase, while the f values for the conventional excited and quasi-exotic states differ by at least an order of magnitude even in the strange case. We note that the zeros visible in the curve for the quasi-exotic state come from a sign change of f .

To close this section we would like to remark that the masses of the meson excitations discussed here are not well-anchored to exact results in QCD. Thus, they can depend rather strongly on the model parameters and do, in general, not compare well to experimental data. Fine-tuning the pa-

rameters can be used to achieve a reasonable description of excited-state masses, but since this is not the focus of our argument herein, we refer the interested reader to our previous studies in this direction [36] and references therein.

Another remark is that changing the model parameters might also change the behavior and role of states with regard to their level ordering, both in terms of quasi-exotic or conventional characteristic as well as the behavior of having real solutions of the homogeneous BSE or not. However, as mentioned above, while states without real solutions of the homogeneous BSE have to be discarded in our present context, our picture and argument are still valid using the remaining states.

5 Orbital angular momentum

While l is not a Lorentz invariant, the covariants in Eq. (1) can be identified with orbital angular momentum l associated with the relative $\bar{q}q$ momentum in the meson's rest

frame [106]. Terms unexpected in a quark-model setup appear due to the fully covariant amplitude, such as P -wave components in the pseudoscalar or vector BSA or S -wave components in the scalar one.

Here, we focus on the comparison of ground states and their excitations including the open-flavor case as they are contained in Fig. 2. The l -content of several key states is presented in Figs. 3 and 4 as well as in Tab. 1 in the following way: the covariants in Eq. (1) are numbered 1 to 4: 1 and 2 correspond to S -wave, 3 and 4 are P -wave. For the vector meson each of these covariants are combined with the two four-vectors γ^μ and k^μ , arriving at a set of eight vector covariants (for details, see, e. g., Ref. [24]), thus numbered 1 to 8. In the vector case, covariants 1 and 2 correspond to S -wave, 3 - 6 are P -wave, and 7 and 8 are D -wave.

After solving the homogeneous BSE, we canonically normalize the BSA and explicitly extract the contributions from each combination of covariants to the norm. The squares of these contributions are plotted in Figs. 3 and 4 with their sum normalized to one. Full details on this kind of construction, the complete sets of covariants as well as the basis for the interpretation in terms of l can be found in Ref. [36].

We start with the discussion of ground states presented in Fig. 3: Next to each other in each row of the figure, we present the key states along the ground-state trajectories as outlined in Fig. 1 and plotted in Fig. 2 for $J^{\mathcal{P}\mathcal{C}} = 0^{-+}, 0^{++}$, and 1^{--} . In this way, the three columns in Fig. 3 contain the flavor combinations $\bar{u}u$, $\bar{u}s$, and $\bar{s}s$, respectively. For easy reference, all numbers corresponding to the bar heights in the figures are collected in Tab. 1.

It is obvious immediately that changes along the trajectory $\bar{u}u \rightarrow \bar{u}s \rightarrow \bar{s}s$ are very small. For example, the pion is more than 80% S -wave and negligible pure P -wave. The same picture holds for the K and a theoretical pure flavor $\bar{s}s$ pseudoscalar ground state. It is important to note here that we always deal with ideally mixed flavor states due to the absence of flavor-mixing or -changing contributions in the RL BSE interaction kernel. This does not mean, however, that an investigation of flavor-mixed states would be impossible at our level of sophistication, since one can always perform mixing at the hadronic level [95]. In fact, we can indeed argue on the basis of our results that any particular mixture of $\bar{u}u$ and $\bar{s}s$ (and, of course, away from the isospin-symmetric limit also $\bar{d}d$) should have an orbital angular momentum content very similar to any of the pure $\bar{f}f$ states for any of the flavors $f = u, d, s$.

Similarly, in the scalar and vector cases, the ground states do not only appear in the l -configuration expected from the quark model [36], but also stay almost unchanged along their trajectories. A few key examples are the $a_0(980)$ with only 7% S -wave, 45% P -wave, and 48% mixed contributions, representative of also the κ , as well as the ρ with 87% S -wave, negligible pure P - and D -wave parts, and a total of

12% of various mixed contributions, also representative of the K^* and the ϕ .

The excited-state results are shown in Fig. 4 for both conventional and exotic excited quarkonia with $J^{\mathcal{P}} = 0^-$ and 0^+ . In particular, the states are extracted in accordance to those shown in Fig. 2 such that the first and third rows in Fig. 4 contain conventional $J^{\mathcal{P}\mathcal{C}}$ excitations while the second and fourth rows show the transitions from exotic to quasi-exotic back to exotic states along the $\bar{u}u \rightarrow \bar{u}s \rightarrow \bar{s}s$ trajectory. Note that on such a trajectory the excitation quantum number n changes due to the increased number of states in a $J^{\mathcal{P}}$ channel, which contains both signs of \mathcal{C} in the respective $J^{\mathcal{P}\mathcal{C}}$ channels.

Table 1 Orbital angular momentum content of states shown in Figs. 3 and 4. Numbers are given in %. Question marks parentheses indicate that the mass of such a state, which would likely be included in the name, is not experimentally known yet as is the case also for other states listed here, e. g., the b_0 , which is an isovector exotic scalar. A l indicates an excitation analog to a radial excitation in the quark model. Flavor subscripts denote ideally mixed components.

Name	$n(J^{PC})$	S	$S-P$	P	$P-D$	D	$S-D$
π	$0(0^{-+})$	81.8	18.2	0.0	—	—	—
K	$0(0^{-})$	85.0	14.9	0.0	—	—	—
$\eta_{\bar{s}s}$	$0(0^{-+})$	90.8	9.1	0.0	—	—	—
$a_0(980)$	$0(0^{++})$	6.6	48.4	45.0	—	—	—
κ	$0(0^+)$	5.5	43.0	51.4	—	—	—
$f_{0\bar{s}s}$	$0(0^{++})$	2.7	28.5	68.8	—	—	—
ρ	$0(1^{--})$	86.7	9.8	1.4	1.9	0.1	0.0
K^*	$0(1^-)$	89.1	8.6	1.0	1.2	0.1	0.0
ϕ	$0(1^{--})$	93.5	5.6	0.4	0.4	0.0	0.0
$\pi(1300)$	$1(0^{-+})$	92.9	6.8	0.3	—	—	—
$K(1460)$	$2(0^-)$	91.9	7.8	0.3	—	—	—
$\eta'_{\bar{s}s}$	$1(0^{-+})$	95.1	4.7	0.2	—	—	—
ρ_0	$0(0^{--})$	91.3	8.6	0.1	—	—	—
$K(?)$	$1(0^-)$	93.6	6.3	0.1	—	—	—
$\omega_{0\bar{s}s}$	$0(0^{--})$	95.6	4.3	0.1	—	—	—
$a_0(1450)$	$1(0^{++})$	0.2	3.8	96.1	—	—	—
$K_0^*(1430)$	$2(0^+)$	2.8	40.9	56.3	—	—	—
$f_{l_{0\bar{s}s}}$	$1(0^{++})$	0.2	4.6	95.2	—	—	—
b_0	$0(0^{+-})$	2.4	21.2	76.3	—	—	—
$K_0^*(?)$	$1(0^+)$	3.0	22.3	74.7	—	—	—
h_0	$0(0^{+-})$	0.9	11.3	87.8	—	—	—

It is remarkable that there is no strong difference between the conventional and exotic excitations in both cases, i. e., the exotic character of the corresponding excited states in our approach does not come about via some kind of excitation in orbital-angular momentum corresponding to the $\bar{q}q$ relative momentum. Rather, it seems to be a mechanism akin to a radial excitation in the quark model. We note again at this point that gluonic excitation mechanisms are not built in explicitly, but implicitly in our approach.

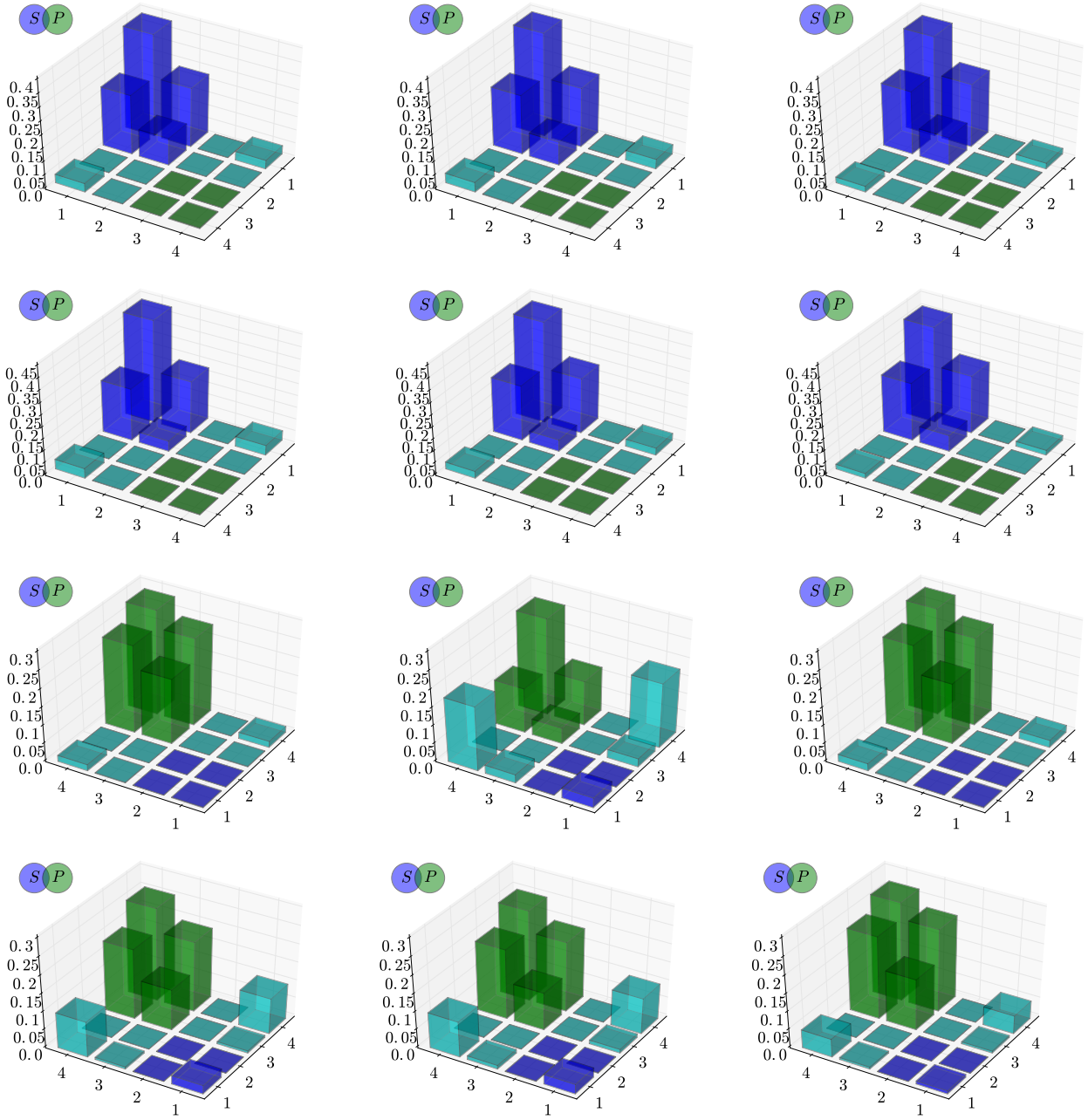


Fig. 4 Orbital angular momentum contributions to the BSA's canonical norm for conventional and exotic excited quarkonia with $J = 0$. The rows in the figure correspond to key points on the graphs in Fig. 2 as follows (states in notation flavor- $n(J^{\mathcal{P}(\mathcal{C})})$): *Upper row*: $\bar{u}u$ -1(0^{+-}), $\bar{u}s$ -2(0^-), $\bar{s}s$ -1(0^{+-}); *Upper center row*: $\bar{u}u$ -0(0^{--}), $\bar{u}s$ -1(0^-), $\bar{s}s$ -0(0^{--}); *Lower center row*: $\bar{u}u$ -1(0^{++}), $\bar{u}s$ -2(0^+), $\bar{s}s$ -1(0^{++}); *Lower row*: $\bar{u}u$ -0(0^{+-}), $\bar{u}s$ -1(0^+), $\bar{s}s$ -0(0^{+-}).

In Fig. 5 we plot an overview of the l contributions together with the values for f on a logarithmic scale for all states shown in Figs. 3 and 4.

6 Charmed strange sector

Open-charm mesons are of particular DCSB relevance [107–111]. We add a small set of results containing the D_s meson

and its first excitation using the slightly different model interaction of Ref. [98]. In particular, this interaction does not have the correct asymptotic behavior of the QCD running coupling, which makes a re-determination of quark masses necessary, which we achieve analogously to the fitting scheme described above for the light-strange meson results. With $\omega = 0.6$ GeV, $D = 1$ GeV², the current-quark masses $m_u = 0.0045$ GeV, $m_s = 0.11$ GeV, and $m_c = 0.97$ GeV are fitted

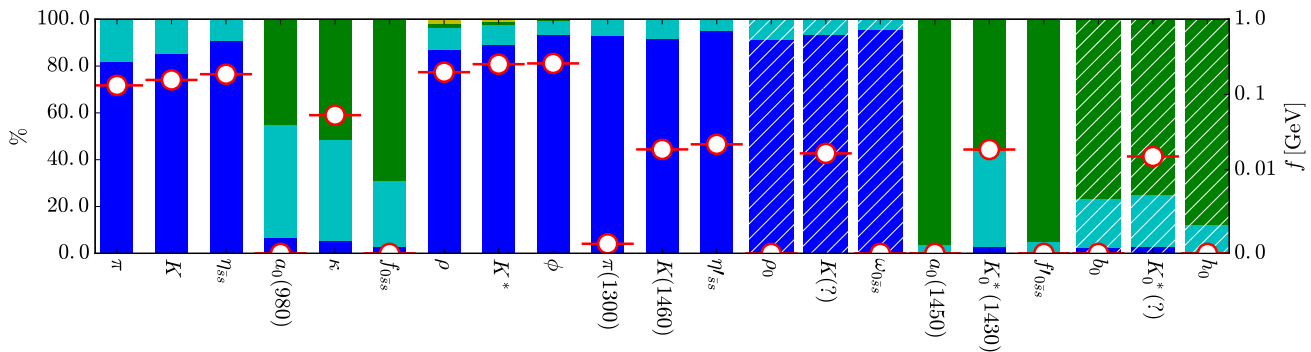


Fig. 5 Orbital angular momentum contributions. Columns labeled by experimental states, where available. Colors: S (blue), P (green), D (red), S - P -mix (cyan), S - D -mix (magenta), P - D -mix (yellow). (Quasi-)exotic bands are wider and hatched. *Overlay* (right vertical axis, linear below 0.01 GeV): leptonic decay constants (red filled circles with lines).

to the π , K , and D -meson masses to yield $M_\pi = 0.137$, $f_\pi = 0.129$, $M_K = 0.499$, and $f_K = 0.157$ GeV as well as $M_D = 1.868$ and $f_D = 0.268$ GeV compared to the experimental $M_{D^+} = 1.86961(9)$ and $f_{D^+} = 0.2046(50)$ GeV [101].

Table 2 Charmed strange results in GeV.

$J^{\mathcal{P}(\mathcal{C})}$	$\bar{s}s$		$\bar{c}s$		$\bar{c}c$	
	M	$ f $	M	$ f $	M	$ f $
$0^{-(+)}$	0.698	0.187	1.888	0.268	2.710	0.342
$0^{-(-)}$	1.427	0.000	2.357	0.180	3.113	0.000

The results for combinations of c and s flavors are given in Tab. 2. Experimentally one has $M_{D_s^+} = 1.9683(1)$ and $f_{D_s^+} = 0.2575(46)$ GeV. The first radial excitation is connected to exotic pseudoscalars for $\bar{c}c$ and $\bar{s}s$, which shows that for large asymmetries regarding the quark masses inside the meson, f is not necessarily a reliable means to distinguish whether experimental states are quasi-exotic or not.

7 Conclusions and outlook

In summary, we argue for the existence of open-flavor analogs of exotic mesons from a quark-bilinear covariant BSA on the basis of the following points:

1. there is no conceptual difference between the construction of exotic and non-exotic quark-bilinear meson states within a Poincare covariant bound-state approach
2. there is no conceptual difference in the construction of an equal-flavor and an open-flavor state
3. based on our OAMD results, the inherent character of such states is not altered along quark-mass changing trajectories depicted in Fig. 1
4. it is reasonable to assume continuity of meson spectra with respect to variations of the quark mass

It is important to note here that including hadronic decay channels in a more sophisticated truncation would certainly

have qualitative impact on the results. However, the central results of our study should be robust with regard to such an extension, since they mainly regard how states with certain properties appear together or in relation to each other. In addition, since our anchoring limits and relations provide exact results in QCD and this should be also the case in any more sophisticated truncation of the DSBSE approach including those where hadronic channels are taken into account, the robustness of the anchor should translate well onto the key results of any more sophisticated study.

To the best of our knowledge, we describe and analyse such quasi-exotic states, as we term them due to their missing restriction in the decisive quantum number \mathcal{C} , for the first time: by continuity with respect to the quark masses they do not exist in the quark model, and a setup like ours has not yet been explored before.

In particular, we have shown how and if, on the basis of a covariant meson amplitude, quasi-exotic mesons can be identified by the order of magnitude of their leptonic decay constants. While the prime example is that of charged quasi-exotic pion excitations, there can be other cases where such an identification is clear and would provide evidence for quasi-exotic states in the open-flavor meson spectrum with clear connections to their exotic quarkonium partners.

Orbital angular $\bar{q}q$ momentum, on the other hand, provides no clues to discern such states in our study. However, the orbital-angular-momentum decomposition of the states investigated here shows clear similarities along the $\bar{u}u \rightarrow \bar{u}s \rightarrow \bar{s}s$ trajectory. This supports the concept of flavor-mixing mechanisms executed at the hadronic level in general, but in particular in the DSBSE approach. In addition it clearly demonstrates the conceptual similarity of exotic and quasi-exotic quark bilinear meson states.

As a result of the correspondence shown between exotic $J^{\mathcal{P}\mathcal{C}}$ and quasi-exotic $J^{\mathcal{P}}$ states, for each flavor combination there should be more states at and above the lowest (quasi)exotic meson mass than expected in the traditional quark model. Next steps to provide a better grasp on quasi-

exotic states include calculations of their hadronic decay properties along the lines of [112, 113].

Acknowledgements We acknowledge helpful conversations with M. Gomez-Rocha. This work was supported by the Austrian Science Fund (FWF) under project no. P25121-N27.

References

1. C. Meyer, Y. Van Haarlem, *Phys.Rev. C* **82**, 025208 (2010)
2. E. Eichten, K. Gottfried, T. Kinoshita, K.D. Lane, T.M. Yan, *Phys. Rev. D* **21**, 203 (1980)
3. S. Godfrey, N. Isgur, *Phys. Rev. D* **32**, 189 (1985)
4. E.J. Eichten, C. Quigg, *Phys. Rev. D* **49**, 5845 (1994)
5. D. Alde, et al., *Phys. Lett. B* **205**, 397 (1988)
6. H. Aoyagi, et al., *Phys. Lett. B* **314**, 246 (1993)
7. D.R. Thompson, et al., *Phys. Rev. Lett.* **79**, 1630 (1997)
8. A. Abele, et al., *Phys. Lett. B* **423**, 175 (1998)
9. A. Abele, et al., *Phys. Lett. B* **446**, 349 (1999)
10. A.R. Dzierba, et al., *Phys. Rev. D* **67**, 094015 (2003)
11. P. Salvini, et al., *Eur. Phys. J. C* **35**, 21 (2004)
12. G.S. Adams, et al., *Phys. Lett. B* **657**, 27 (2007)
13. M. Alekseev, et al., *Phys. Rev. Lett.* **104**, 241803 (2010)
14. M. Lu, et al., *Phys. Rev. Lett.* **94**, 032002 (2005)
15. J. Kuhn, et al., *Phys. Lett. B* **595**, 109 (2004)
16. E.I. Ivanov, et al., *Phys. Rev. Lett.* **86**, 3977 (2001)
17. G.S. Adams, et al., *Phys. Rev. Lett.* **81**, 5760 (1998)
18. A.R. Dzierba, et al., *Phys. Rev. D* **73**, 072001 (2006)
19. R.A. Briceno, et al., *Chin. Phys.* **C40**(4), 042001 (2016)
20. C.J. Burden, M.A. Pichowsky, *Few-Body Syst.* **32**, 119 (2002)
21. N. Hu, et al., *Acta Sci. Naturalium Universitatis Pekinensis* **12**, 213 (1966)
22. N. Hu, et al., *Acta Sci. Naturalium Universitatis Pekinensis* **12**, 209 (1966)
23. C.H. Llewellyn-Smith, *Ann. Phys.* **53**, 521 (1969)
24. A. Krassnigg, M. Blank, *Phys. Rev. D* **83**, 096006 (2011)
25. P. Maris, C.D. Roberts, *Phys. Rev. C* **56**, 3369 (1997)
26. T.U. Hilger, *Medium Modifications of Mesons*. Ph.D. thesis, TU Dresden (2012)
27. C.S. Fischer, S. Kubrak, R. Williams, *Eur. Phys. J. A* **50**, 126 (2014)
28. E. Rojas, B. El-Bennich, J. de Melo, *Phys. Rev. D* **90**, 074025 (2014)
29. S. Leita, A. Stadler, M.T. Pena, E.P. Biernat, *Phys. Lett. B* **764**, 38 (2017)
30. T. Hilger, A. Krassnigg, *EPJ Web Conf.* **137**, 01010 (2017)
31. T. Hilger, M. Gómez-Rocha, A. Krassnigg, W. Lucha, arXiv:1702.06262 (2017)
32. C.J. Burden, L. Qian, C.D. Roberts, P.C. Tandy, M.J. Thomson, *Phys. Rev. C* **55**, 2649 (1997)
33. P. Watson, W. Cassing, P.C. Tandy, *Few-Body Syst.* **35**, 129 (2004)
34. A. Krassnigg, *Phys. Rev. D* **80**, 114010 (2009)
35. C.S. Fischer, S. Kubrak, R. Williams, *Eur. Phys. J. A* **51**, 10 (2015)
36. T. Hilger, M. Gomez-Rocha, A. Krassnigg, arXiv:1508.07183 (2015)
37. J.J. Dudek, *Phys. Rev. D* **84**, 074023 (2011)
38. J.J. Dudek, R.G. Edwards, M.J. Peardon, D.G. Richards, C.E. Thomas, *Phys. Rev. D* **82**, 034508 (2010)
39. J.J. Dudek, R.G. Edwards, P. Guo, C.E. Thomas, *Phys. Rev. D* **88**(9), 094505 (2013)
40. D. Horn, J. Mandula, *Phys. Rev. D* **17**, 898 (1978)
41. N. Isgur, J.E. Paton, *Phys. Rev. D* **31**, 2910 (1985)
42. R.L. Jaffe, K. Johnson, Z. Ryzak, *Annals Phys.* **168**, 344 (1986)
43. T. Barnes, F.E. Close, F. de Viron, J. Weyers, *Nucl. Phys. B* **224**, 241 (1983)
44. M.S. Chanowitz, S.R. Sharpe, *Nucl. Phys. B* **222**, 211 (1983)
45. I.J. General, S.R. Cotanch, F.J. Llanes-Estrada, *Eur. Phys. J. C* **51**, 347 (2007)
46. P. Guo, A.P. Szczepaniak, G. Galata, A. Vassallo, E. Santopinto, *Phys. Rev. D* **78**, 056003 (2008)
47. W. Chen, R. Kleiv, T. Steele, B. Bulthuis, D. Harnett, et al., *JHEP* **1309**, 019 (2013)
48. S.R. Cotanch, F.J. Llanes-Estrada, *Fizika B* **20**, 1 (2011)
49. M. Blank, A. Krassnigg, *Phys. Rev. D* **84**, 096014 (2011)
50. C. Popovici, T. Hilger, M. Gomez-Rocha, A. Krassnigg, *Few Body Syst.* **56**(6), 481 (2015)
51. T. Hilger, C. Popovici, M. Gomez-Rocha, A. Krassnigg, *Phys. Rev. D* **91**, 034013 (2015)
52. T. Hilger, M. Gomez-Rocha, A. Krassnigg, *Phys. Rev. D* **91**, 114004 (2015)
53. S.X. Qin, L. Chang, Y.X. Liu, C.D. Roberts, D.J. Wilson, *Phys. Rev. C* **85**, 035202 (2012)
54. C.S. Fischer, *J. Phys. G* **32**, R253 (2006)
55. C.D. Roberts, S.M. Schmidt, *Prog. Part. Nucl. Phys.* **45**, S1 (2000)
56. M. Blank, A. Krassnigg, *Phys. Rev. D* **82**, 034006 (2010)
57. D. Horvatic, D. Blaschke, D. Klabucar, O. Kaczmarek, *Phys. Rev. D* **84**, 016005 (2011)
58. G. Eichmann, C.S. Fischer, C.A. Welzbacher, *Phys. Rev. D* **93**(3), 034013 (2016)

59. Z.F. Cui, I.C. Cloët, Y. Lu, C.D. Roberts, S.M. Schmidt, S.S. Xu, H.S. Zong, *Phys. Rev. D* **94**, 071503 (2016)
60. F. Gao, Y.x. Liu, *Phys. Rev. D* **94**(7), 076009 (2016)
61. F. Gao, Y.x. Liu, *Phys. Rev. D* **94**(9), 094030 (2016)
62. A. Bender, W. Detmold, C.D. Roberts, A.W. Thomas, *Phys. Rev. C* **65**, 065203 (2002)
63. M.S. Bhagwat, A. Höll, A. Krassnigg, C.D. Roberts, P.C. Tandy, *Phys. Rev. C* **70**, 035205 (2004)
64. M. Gomez-Rocha, T. Hilger, A. Krassnigg, *Few Body Syst.* **56**(6), 475 (2015)
65. M. Gomez-Rocha, T. Hilger, A. Krassnigg, *Phys. Rev. D* **92**(5), 054030 (2015)
66. M. Gomez-Rocha, T. Hilger, A. Krassnigg, *Phys. Rev. D* **93**, 074010 (2016)
67. L. Chang, C.D. Roberts, *Phys. Rev. Lett.* **103**, 081601 (2009)
68. H. Sanchis-Alepuz, R. Williams, *Phys. Lett. B* **749**, 592 (2015)
69. H. Sanchis-Alepuz, R. Williams, *J. Phys. Conf. Ser.* **631**(1), 012064 (2015)
70. W.J. Marciano, H. Pagels, *Phys. Rept.* **36**, 137 (1978)
71. T. Maskawa, H. Nakajima, *Prog. Theor. Phys.* **52**, 1326 (1974)
72. K.I. Aoki, M. Bando, T. Kugo, M.G. Mitchard, H. Nakatani, *Prog. Theor. Phys.* **84**, 683 (1990)
73. T. Kugo, M.G. Mitchard, *Phys. Lett. B* **282**, 162 (1992)
74. M. Bando, M. Harada, T. Kugo, *Prog. Theor. Phys.* **91**, 927 (1994)
75. H.J. Munczek, *Phys. Rev. D* **52**, 4736 (1995)
76. E.P. Biernat, M.T. Peña, J.E. Ribeiro, A. Stadler, F. Gross, *Phys. Rev. D* **90**(9), 096008 (2014)
77. P. Maris, C.D. Roberts, P.C. Tandy, *Phys. Lett. B* **420**, 267 (1998)
78. C.A. Dominguez, *Phys. Rev. D* **15**, 1350 (1977)
79. C.A. Dominguez, *Phys. Rev. D* **16**, 2313 (1977)
80. M.K. Volkov, V.L. Yudichev, *Phys. Part. Nucl.* **31**, 282 (2000)
81. A. Höll, A. Krassnigg, C.D. Roberts, *Phys. Rev. C* **70**, 042203(R) (2004)
82. A. Höll, A. Krassnigg, C.D. Roberts, [arXiv:nucl-th/0311033](https://arxiv.org/abs/nucl-th/0311033) (2003)
83. C. McNeile, C. Michael, *Phys. Lett. B* **642**, 244 (2006)
84. E.V. Mastropas, D.G. Richards, *Phys. Rev. D* **90**(1), 014511 (2014)
85. A. Ballon-Bayona, G. Krein, C. Miller, *Phys. Rev. D* **91**, 065024 (2015)
86. G. Krein, *J. Phys. Conf. Ser.* **706**(4), 042004 (2016)
87. M.S. Bhagwat, A. Höll, A. Krassnigg, C.D. Roberts, *Nucl. Phys. A* **790**, 10 (2007)
88. P. Maris, P.C. Tandy, *Phys. Rev. C* **60**, 055214 (1999)
89. A. Krassnigg, *PoS CONFINEMENT8*, 075 (2008)
90. S.M. Dorkin, T. Hilger, L.P. Kaptari, B. Kämpfer, *Few Body Syst.* **49**, 247 (2011)
91. S.M. Dorkin, L.P. Kaptari, T. Hilger, B. Kämpfer, *Phys. Rev. C* **89**, 034005 (2014)
92. A. Krassnigg, C.D. Roberts, *Fizika B* **13**, 143 (2004)
93. M. Blank, A. Krassnigg, *Comput. Phys. Commun.* **182**, 1391 (2011)
94. T. Hilger, *Phys. Rev. D* **93**, 054020 (2016)
95. A. Höll, A. Krassnigg, C.D. Roberts, S.V. Wright, *Int. J. Mod. Phys. A* **20**, 1778 (2005)
96. A. Krassnigg, M. Gomez-Rocha, T. Hilger, *J. Phys.: Conf. Ser.* **742**(1), 012032 (2016)
97. A. Krassnigg, C.D. Roberts, *Nucl. Phys. A* **737**, 7 (2004)
98. R. Alkofer, P. Watson, H. Weigel, *Phys. Rev. D* **65**, 094026 (2002)
99. M.S. Bhagwat, M.A. Pichowsky, P.C. Tandy, *Phys. Rev. D* **67**, 054019 (2003)
100. G. Eichmann, H. Sanchis-Alepuz, R. Williams, R. Alkofer, C.S. Fischer, *Prog. Part. Nucl. Phys.* **91**, 1 (2016)
101. K.A. Olive, others (Particle Data Group), *Chin. Phys. C* **38**, 090001 (2014)
102. G. Eichmann, C.S. Fischer, H. Sanchis-Alepuz, *Phys. Rev. D* **94**(9), 094033 (2016)
103. G. Eichmann, *Few Body Syst.* **58**(2), 81 (2017)
104. M.S. Bhagwat, A. Höll, A. Krassnigg, C.D. Roberts, S.V. Wright, *Few-Body Syst.* **40**, 209 (2007)
105. M. Blank, A. Krassnigg, *AIP Conf. Proc.* **1343**, 349 (2011)
106. M.S. Bhagwat, A. Krassnigg, P. Maris, C.D. Roberts, *Eur. Phys. J. A* **31**, 630 (2007)
107. T. Hilger, R. Thomas, B. Kämpfer, *Phys. Rev. C* **79**, 025202 (2009)
108. T. Hilger, B. Kämpfer, S. Leupold, *Phys. Rev. C* **84**, 045202 (2011)
109. T. Buchheim, T. Hilger, B. Kämpfer, *Phys. Rev. C* **91**, 015205 (2015)
110. R. Rapp, et al., *Lect. Notes Phys.* **814**, 335 (2011)
111. T. Buchheim, T. Hilger, B. Kämpfer, *J. Phys. Conf. Ser.* **668**(1), 012047 (2016)
112. D. Jarecke, P. Maris, P.C. Tandy, *Phys. Rev. C* **67**, 035202 (2003)
113. V. Mader, G. Eichmann, M. Blank, A. Krassnigg, *Phys. Rev. D* **84**, 034012 (2011)